ROYAL SOCIETY OF CHEMISTRY

PAPER

CrossMark
click for updates

Effect of surfactants, pH and water hardness on the surface properties and agglomeration behavior of engineered TiO$_2$ nanoparticles

Frédéric Loosli* and Serge Stoll*

The influence of sodium dodecyl sulfate (SDS) on the stability of TiO$_2$ engineered nanoparticle (ENP) dispersions is investigated under various pH conditions, SDS and divalent cation concentrations. Based on different scenarios and systematic measurements of surface charges and z-average sizes, a detailed mechanistic approach is proposed assuming surfactant adsorption/desorption, charge inversion, cation bridging, specific adsorption, hydrophobic effects, agglomeration and disagglomeration. Adsorption of SDS on oppositely charged TiO$_2$ nanoparticles is found to strongly modify their stability. Formation of large agglomerates can be achieved *via* several routes: i) in the absence of SDS and by adjusting the pH close to the TiO$_2$ point of zero charge, and ii) in the presence of SDS at a concentration where the positive surface charges of the TiO$_2$ nanoparticles are counterbalanced by the SDS negative charges (charge neutralization). It is also found that hydrophobic interaction mechanisms between the SDS molecules can also promote the formation of large structures. The influence of pH variations on TiO$_2$–SDS electrostatic complexes, formed at low pH, indicates that an excess of SDS is required to prevent the formation of large agglomerates upon pH changes. At low or intermediate SDS concentrations, TiO$_2$ stability is governed by the subtle interplay of SDS adsorption and TiO$_2$ surface charge acid–base properties. The presence of divalent electrolytes (water hardness) is found to reduce the SDS amount adsorbed on TiO$_2$ ENPs and to promote the formation of large micron-sized agglomerates by cation bridging. Our results also indicate that the dispersion preparation protocol is an important issue to consider when ENPs and SDS mixtures have to be prepared and that for the formation of "individually" coated and stable nanoparticles, punctual addition of SDS is required at concentrations higher than the isoelectric point.

Environmental significance

Relatively little attention has been paid to date to the impact of surfactant molecules on the stability of manufactured nanoparticles in aquatic systems and the detailed mechanistic approach based on different scenarios and systematic measurements. In this study we demonstrate that surfactant molecules can significantly influence the TiO$_2$ nanoparticle stability through several processes including surface adsorption and agglomeration. These processes are found reversible (desorption, disagglomeration) by changing the pH or SDS concentration. The surfactant concentration, mixing procedure (successive or punctual addition), pH as well as the presence of divalent electrolytes are also found to be of high importance. Stabilization/destabilization processes are shown here to be governed by complex mechanisms such as electrostatic repulsions, hydrophobic interactions between SDS chains, specific adsorption of divalent electrolytes, adsorption/desorption of surfactant molecules, and cation bridging. It should be also noted that for a given SDS concentration, electrostatic TiO$_2$–SDS complexes can undergo important transformation with pH. We believe that this study is of high value for i) the establishment of ENP dispersion protocols to improve nanoparticle stability with the use of surfactant molecules, ii) a better understanding of ENP commercial dispersions stabilized by surfactants in contact with environmental matrices, iii) the understanding of the impact of water hardness on the SDS–TiO$_2$ nanoparticle interactions in particular by considering the competition between the divalent cations and the surfactant molecules and iv) for risk assessment evaluation of ENPs entering aquatic systems where both changes in pH and water hardness are expected.

1. Introduction

Group of Environmental Physical Chemistry, F.-A. Forel Institute, Section des Sciences de la Terre et de l'Environnement, University of Geneva, 66 boulevard Carl-Vogt, CH-1211 Genève 4, Switzerland. E-mail: looslifred@gmail.com, serge.stoll@unige.ch; Fax: +41 22 379 0302; Tel: +41 22 379 0341, +41 22 379 0333

Due to their very unique properties,[1] mainly arising from their huge specific surface area in comparison with bulk materials, engineered nanoparticles (ENPs) are nowadays used not only in many domains such as biomedicine, textile and cosmetic industries but also in the development of sensors

This journal is © The Royal Society of Chemistry 2017

Environ. Sci.: Nano, 2017, 4, 203–211 | 203

and electronic devices.[2–4] ENPs are produced in continuously increasing quantities to meet the needs of industry.[5,6] One of the most produced nanomaterials, with more than 10 000 tons per year,[7] is TiO_2 due to its numerous applications and high stability.[2,8–12] The stability of ENPs, which is often required for industrial applications, is strongly dependent on water chemistry such as pH and ionic strength[13–15] and the presence of various compounds in the dispersion media.[16–18] An important group of chemicals that are often used to stabilize ENPs during synthesis are surfactants.[19–21] These amphiphilic compounds have the ability to self-assemble into well-defined structures, modify interfaces, improve dispersion stability and are frequently used for the synthesis of many inorganic nanomaterials.[22,23] Surfactants are found in detergents, personal care, washing and cleaning agents as well as in numerous technical applications such as textile auxiliaries, agrochemicals, the metal and mining industry, the plastic industry and lubricants.[24] According to the European surfactant producers statistics the total quantity of surfactants produced in 2013 in Western Europe was 2.9 million tons.[25] Surfactants are also used as efficient compounds for the removal of heavy metals present in water *via* surfactant-based separation processes such as micellar-enhanced ultrafiltration.[26,27] Only a few systematic studies were made to evaluate in a systematic way the stability of ENPs in the presence of surfactants. The role of the surfactant on the stability of TiO_2 particles was first investigated by Imae *et al.*[28] They studied the interaction between surfactants at concentrations above the CMC and TiO_2 ENPs using absorbance, dynamic light scattering measurements and electron microscope observations. They attributed the change of absorbance in the presence of the surfactant to different adsorption modes of hemimicelles or double layer compression depending on the TiO_2 surface charge pH dependence and showed that the presence of trivalent cations strongly influences the TiO_2 stability and induces an arrangement of the double-layer compression. Arnold *et al.* investigated the adsorption of ionic surfactants on hydrophobic particles.[29] This study provided a comparison of surfactant micellization in solution and agglomerate formation at one interface by considering hydrophobic and electrostatic interactions. Liu *et al.* investigated the stability of nano-SiO_2 in the presence of a cationic surfactant[30] and demonstrated that different mechanisms of ENP agglomeration (charge neutralization, depletion flocculation and hydrophobic effects) were involved in the ENP destabilization. Coagulation–flotation processes of inorganic ENPs in the presence of cationic surfactants were also investigated to optimize the removal of ENPs through particle agglomeration for the treatment of wastewaters from industries producing silica ENPs.[31–33] Other studies dealing with ENP–surfactant interactions investigated the structures formed during the complexation processes between bare (or polymer coated) ENPs and surfactants by using Fourier transform infrared spectroscopy,[34] small-angle neutron scattering[35–37] and solvent relaxation nuclear magnetic resonance.[38] In these studies, the authors observed that the presence of surfactants promoted the desorption of the polymer coating due to the conformational change of the polymer layer to a more diffuse state.

Since surfactants are largely used in the field of nanotechnology they are likely to be one of the chemicals that will co-exist with ENPs in the environment. Indeed ENPs have the possibility to contaminate water treatment plants, in which surfactants are present, as well as aquatic systems through direct, indirect, accidental or deliberate ENP release.[39–41] Current knowledge suggests that ENPs entering aquatic systems will exhibit transport and fate behavior that will be highly dependent both on their released form and on the physicochemical characteristics of the receiving water.[42–46] There is thus a great need to evaluate the effects of water chemistry, changing conditions, and stability of the complexes they form with surfactants under environmental conditions.

In this study, we are investigating the properties and stability of TiO_2 ENPs in the presence of sodium dodecyl sulfate (SDS) which is a common anionic surfactant with low production cost.[47] We first focus on the effect of the SDS concentration (and how SDS is added into the ENP dispersions, *i.e.* punctual *versus* successive additions) on TiO_2 stability in a pH domain where electrostatic interactions between the two compounds are favored. Formation of electrostatic complexes based on electrostatic attractions is of great importance for the synthesis of stable ENP dispersions *via* surfactant surface coating. Then, the TiO_2 stability in the presence of SDS, by considering surface charge and size changes, is evaluated upon pH variations and in the presence of divalent cations to investigate the effects of water hardness. This enables the release and behavior of surfactant coated, stable, ENP dispersions in natural waters to be mimicked, which is of high importance for the risk assessment associated with ENPs entering aquatic systems. The novelty of this study is to consider here different scenarios (SDS concentration variations, pH changes, the presence of divalent cations) and systematic measurements of surface charges and *z*-average sizes to propose a detailed mechanistic approach and predict the TiO_2 behavior from pristine solutions to aquatic systems in the presence (or not) of surfactants. The importance of electrostatic and hydrophobic interactions, SDS desorption and specific adsorption of divalent cations is here discussed by considering stabilization, agglomeration and disagglomeration processes.

2. Materials and methods

2.1. Materials

1 g L^{-1} dispersions were prepared by dispersing anatase TiO_2 ENP powder (Nanostructured & Amorphous Material Inc, Houston, TX, USA) in ultrapure Milli Q water (Millipore, Zoug, ZG, Switzerland, with $R > 18$ MΩ cm, T.O.C. < 2 ppb). The pristine diameter and specific surface area were, as given by the manufacturer, equal to 15 nm (TEM) and 240 m^2 g^{-1} (BET). The dispersions were sonicated with an ultrasonic probe (CV18, Sonics Vibra cell, Blanc Labo S.A., Switzerland)

delivering a power of 50 W for 15 min using a pulsed 80% mode.[48] Sodium dodecyl sulfate (AppliChem, purity >99%, Darmstadt, Germany) solutions were prepared by dissolving the surfactant in ultrapure Milli Q water and used without further purification. To adjust the dispersion pH, sodium hydroxide and hydrochloric acid (1 M NaOH or HCl, Titrisol®, Merck, Zoug, ZG, Switzerland) were used after dilution. Calcium chloride ($CaCl_2$, purum, Fluka, Buchs, SG, Switzerland) and magnesium chloride ($MgCl_2$, puriss, Sigma Aldrich, Buchs, SG, Switzerland) were used to adjust the electrolyte concentration to the desired values. Experiments were performed in 25 × 90 mm polypropylene tubes (Milian, Vernier, GE, Switzerland) with one 8 × 10 mm crosshead magnetic stirrer (VWR, Nyon, VD, Switzerland) and the agitation speed was set to 500 rpm.

2.2. Zeta potential and size distribution measurements

Determination of z-average hydrodynamic diameters and zeta (ζ) potential values was achieved by dynamic light scattering and laser doppler velocimetry using a Zetasizer Nano ZS instrument (Malvern Instruments, Worcestershire, UK). The Smoluchowski approximation model[49,50] was applied for ζ potential determination. Analysis was conducted at 25 °C and by considering in most cases 50 mg L^{-1} TiO_2 dispersions. Such a concentration was selected to provide an optimum light scattering signal. All polydispersity indexes were found below 0.6. All measurements were made 30 min after pH changes or SDS addition.

2.3. Experiments under pH changing conditions and in the presence of divalent electrolytes

The influence of pH changes (from acidic to circumneutral pH, representative of natural aquatic systems) in the presence of divalent cations on the stability of TiO_2–SDS complexes was investigated by first forming stable complexes at low pH. Then they were introduced into a synthetic water containing divalent cations so as to take into account water hardness. The Ca^{2+} and Mg^{2+} concentrations were, after addition of TiO_2–SDS complexes, equal to 45 mg L^{-1} and 5 mg L^{-1}, the pH to 8.2 and the TiO_2 concentration to 25 mg L^{-1}. The total hardness and pH of investigation were adjusted to the values generally found in the Geneva Lake (France, Switzerland).

2.4. Procedure of SDS addition: punctual addition and successive addition

The effect of the SDS surfactant on the stability of TiO_2 ENPs is investigated for two different scenarios of SDS addition. For "punctual" addition, the total amount of SDS is injected into the TiO_2 dispersion in a unique manner so that the final SDS concentration is directly obtained after the addition. For "successive" addition, the ENP dispersion is titrated with the SDS solution to finally reach, after a certain number of injections, the final desired SDS concentration. The time between each successive addition was set to 30 min which corre-

sponds here to the time needed to obtain a plateau in terms of zeta potential and hydrodynamic diameter values.

3. Results and discussion

TiO_2 characterization. The TiO_2 z-average diameters and ζ potential values as a function of pH for a 50 mg L^{-1} TiO_2 dispersion are shown in Fig. 1. The ζ potential values continuously decrease from +36 mV at pH 3 to −40 mV at pH 11. The point of zero charge (PZC) is found for a pH value equal to 6.1 ± 0.1 which is in good agreement with previous studies.[51,52] For pH values below 5, the TiO_2 ENPs are stable with constant z-average diameters equal to 402 ± 29 nm (mean of triplicate measurements ± standard deviation of mean values). In the pH 5.0 to 7.2 domain strong destabilization of the ENPs occurs and maximum agglomeration is observed for pH values close to the PZC with agglomerate sizes up to 1 μm. This destabilization domain corresponds to ζ potential values in a range of about +20 mV to about −20 mV. At higher pH values (pH > 7.2) the TiO_2 ENP z-average diameters are constant with values equal to 365 ± 8 nm. Even under pH conditions which promote the TiO_2 dispersion state (pH < 5.0 and pH > 7.2) ENPs form agglomerates with sizes significantly larger than their initial pristine diameters (380 nm in comparison with 15 nm). Such a size difference is due to the difficulties to completely disperse as individual objects the TiO_2 ENPs during the solution preparation procedure and irreversible ENP aggregation that happens during ENP storage.[53]

SDS characterization. Due to the presence of sulfate functional groups, SDS molecules exhibit a negative charge in the full pH domain (from 3 to 10) as shown in Fig. 2a where ζ potential values as a function of pH are reported for a 1 g L^{-1} SDS solution. The ζ potential values are found constant and equal to −54.7 ± 3.3 mV. SDS solution conductivity
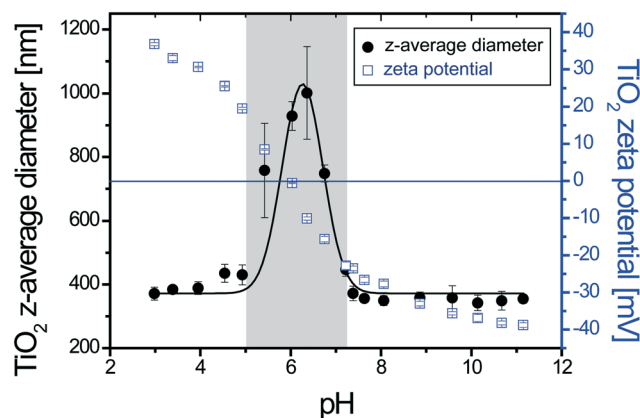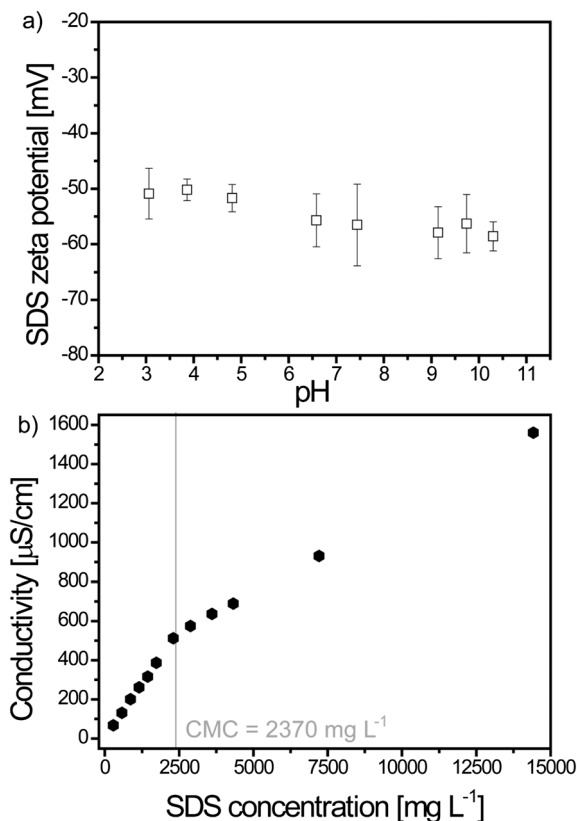

Fig. 1 TiO_2 ENP z-average diameters and ζ potential values as a function of pH. The ENPs are found stable at pH < 5.0 and pH > 7.2 with hydrodynamic diameters around 380 nm, whereas for ζ potential values from +20 mV to −20 mV (5.0 < pH <7.2) strong destabilization occurs resulting in the formation of agglomerates with sizes up to one micron. The point of zero charge (PZC) is found here equal to 6.1 ± 0.1.
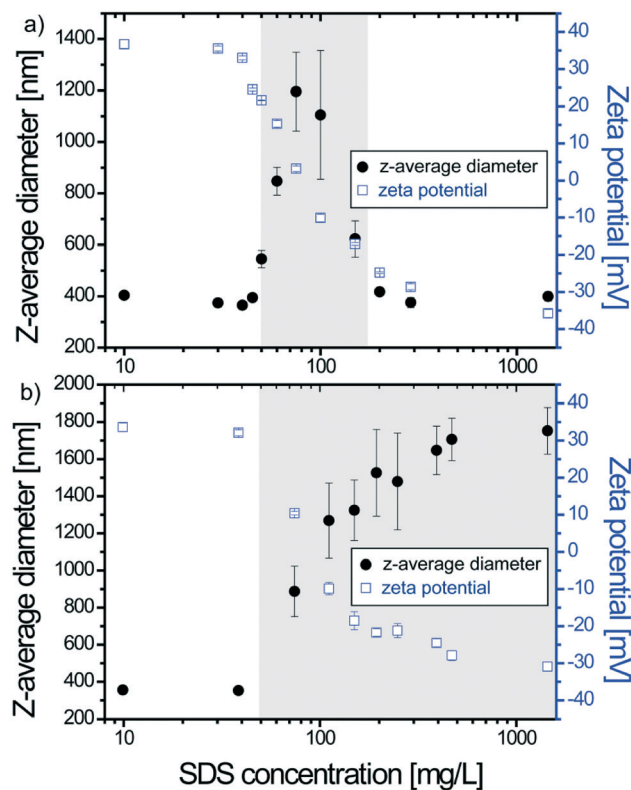
This journal is © The Royal Society of Chemistry 2017

Environ. Sci.: Nano, 2017, 4, 203–211 | 205

Fig. 2 a) ζ potential value of a 1 g L^{-1} SDS solution as a function of pH. SDS is negatively charged in the full pH range due to the presence of the sulfate functional groups. b) SDS critical micelle concentration (CMC) obtained by measuring the variation of the solution conductivity as a function of the SDS concentration at 25 °C. The slope change indicates the formation of micelles. The CMC is found equal to 2370 mg L^{-1}.

Fig. 3 a) Z-average diameter and ζ potential values of a 50 mg L^{-1} TiO$_2$ dispersion at pH 3.1 as a function of SDS concentrations for punctual additions. For SDS concentrations between 50 mg L^{-1} and 150 mg L^{-1} (+20 mV > ζ potential > −20 mV) the ENPs form large agglomerates especially for SDS concentrations with values close to the IEP (+10 mV > ζ potential > −10 mV) with agglomerate sizes larger than 1 μm. b) Z-average diameter and ζ potential values of a 50 mg L^{-1} TiO$_2$ dispersion at pH 3.1 as a function of the SDS concentration obtained for successive SDS additions with 30 minutes between two successive additions. Once agglomerates are formed, further SDS addition does not disagglomerate the ENPs through electrostatic repulsions or steric effects. Destabilization domains are represented by the gray area.

measurement as a function of the SDS concentration in Fig. 2b allows a graphical determination of the critical micellization concentration (CMC) which is found equal to 2.37 g L^{-1} in good agreement with previous studies.[54,55]

3.1. Influence of SDS concentration on TiO$_2$ ENP properties: Punctual *versus* successive addition of SDS

The influence of the SDS concentration on the stability of 50 mg L^{-1} TiO$_2$ dispersions is first investigated at pH 3.1 under conditions where the ENP surfaces are, prior SDS addition, positively charged (Fig. 1) with a ζ potential value equal to +36 mV. All SDS concentrations used during the experiments are below the CMC and two mixing modes are considered (punctual *versus* successive SDS addition).

Punctual SDS additions. ζ potential values and *z*-average diameters as a function of SDS concentrations are represented in Fig. 3a. When SDS concentrations are lower than 50 mg L^{-1} the ENP surface charge is modified due to SDS adsorption but the ζ potential value remains higher than +20 mV. ENPs are stable with constant *z*-average diameter values (385 ± 19 nm). For SDS concentrations between 50 and 150
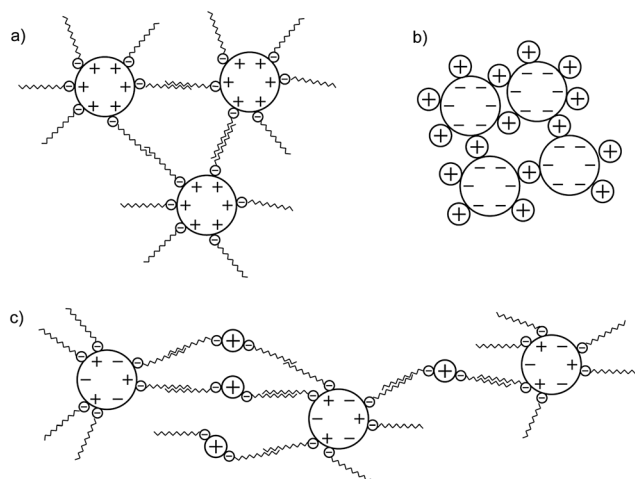
mg L^{-1} adsorption of SDS promotes TiO$_2$ agglomeration. SDS induces TiO$_2$ surface charge neutralization at a concentration equal to 80 mg L^{-1} which corresponds to the ENP–SDS complex isoelectric point (IEP) and to maximum agglomeration with the formation of 1200 nm agglomerates. For higher SDS concentrations (≥200 mg L^{-1}) charge inversion is obtained with ζ potentials higher than −20 mV. Under such conditions, ENPs are found stable again with constant *z*-average diameters equal to 397 ± 22 nm. It is assumed that large agglomerates formed near the IEP in the presence of SDS involved not only different destabilization mechanisms such as charge neutralization but also hydrophobic interactions between SDS tails as suggested by Liu *et al.*[30] and represented in Fig. 4a.

Successive SDS additions. TiO$_2$ ENP stability was also investigated by successively adding SDS to a 50 mg L^{-1} TiO$_2$ dispersion. The corresponding size and ζ potential values after successive SDS additions at pH 3.1 with a 30 min equilibrium time between SDS additions (time needed to obtain constant

206 | *Environ. Sci.: Nano*, 2017, **4**, 203–211

This journal is © The Royal Society of Chemistry 2017

Fig. 4 Schematic representations of TiO_2 and SDS interactions and agglomerate formation. a) TiO_2–SDS agglomerates at pH 3.1. Hydrophobic interactions promote the formation of large agglomerates. b) TiO_2 agglomerate formation at pH 8.2 in the presence of divalent cations (⊕). Cation bridging between TiO_2 promotes agglomeration. c) TiO_2–SDS agglomeration in the presence of divalent cations at pH 8.2. Cation bridging between SDS tails destabilizes the complexes and promotes agglomeration. Length scales of ENPs, SDS chains and divalent cations are not indicated for the sake of clarity.

z-average diameter and ζ potential values for "punctual" SDS additions) are represented in Fig. 3b. For SDS concentrations higher than 50 mg L^{-1} and when large micrometer agglomerates are formed, it is found, contrary to punctual SDS addition, that further SDS addition does not lead to disagglomeration of the agglomerates which were formed at the IEP. This is an important outcome indicating that i) preparation protocols are important parameters to consider when ENPs and SDS mixtures have to be prepared, ii) for the formation of "individually" coated and stable ENPs, punctual addition of SDS is required at concentrations higher than the IEP and iii) once formed agglomerates are relatively resistant to disagglomeration.

3.2. Behavior of SDS–TiO$_2$ complexes upon pH variation

The effect of pH variation (from acid to basic pH with 30 min between successive pH adjustments) on stable SDS–TiO$_2$ electrostatic complexes formed at pH 3.1 is now investigated at a constant TiO_2 concentration (50 mg L^{-1}) and by considering three SDS concentrations. The first concentration is equal to 40 mg L^{-1} and results in the formation of positively charged complexes at pH 3.1. The second one is equal to 200 mg L^{-1} and results in the formation of negatively charged complexes. The third concentration corresponds to 1442 mg L^{-1} and corresponds to the formation of negatively charged complexes with a large excess of SDS.

As shown in Fig. 5a when partial coating of TiO_2 is obtained at 40 mg L^{-1} the increase of pH to 5.5 does not affect the complex stability (constant z-average diameters) even
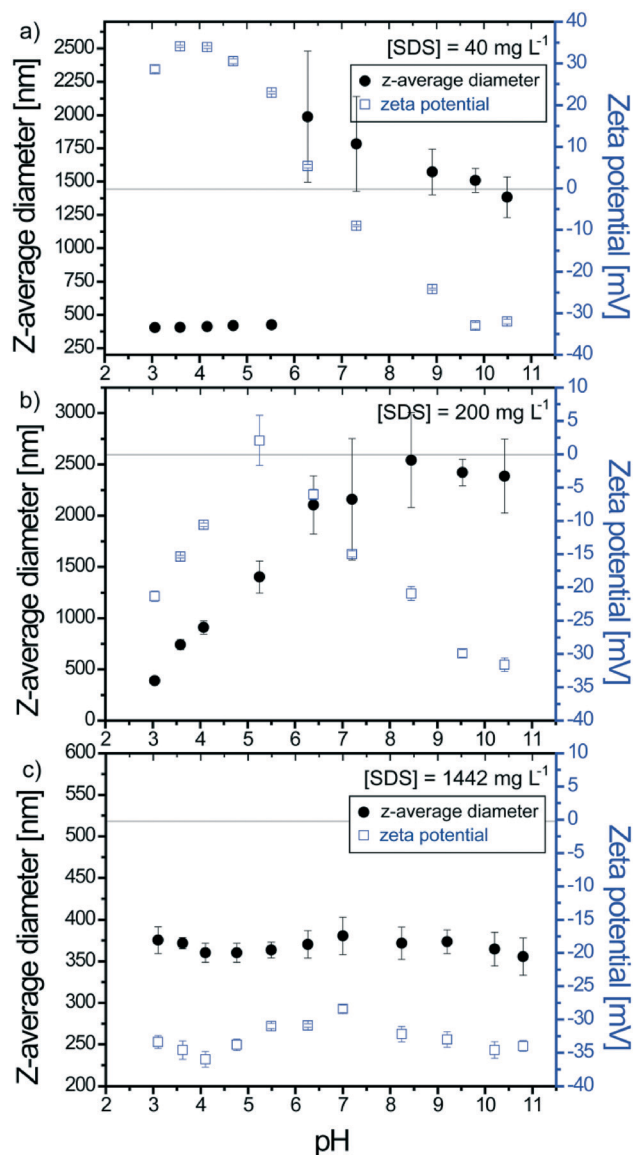
Fig. 5 Z-average diameters and ζ potential values as a function of pH (successive adjustment) for three different SDS concentrations. a) For a 40 mg L^{-1} SDS concentration charge neutralization and inversion is observed. SDS–TiO$_2$ complex properties are mainly controlled by the TiO_2 surface properties. b) For [SDS] = 200 mg L^{-1} the impact of SDS properties on the behavior of the TiO$_2$–SDS complexes is more pronounced. Charge neutralization occurs and the IEP is obtained at pH 5.2. Then by increasing further the pH negative values are obtained due to surface deprotonation. c) For a SDS concentration equal to 1442 mg L^{-1} the SDS–TiO$_2$ complexes exhibit stable z-average diameter and ζ potential values in the full pH range. [TiO$_2$] = 50 mg L^{-1}.

if the deprotonation of TiO_2 hydroxyl surface sites results in a decrease of the ζ potential from +30 mV to +25 mV. Further pH increase rapidly promotes surface charge neutralization then formation of agglomerates (sizes >1 μm). Agglomerate formation is expected to be due here mainly to TiO_2 surface charge neutralization owing to the limited number of adsorbed SDS molecules. It is noteworthy that the IEP is found equal to pH 6.5 ± 0.1 which is higher than the PZC

This journal is © The Royal Society of Chemistry 2017

Environ. Sci.: Nano, 2017, **4**, 203–211 | **207**

value obtained in the absence of SDS (pH_{PZC} = 6.1). Such a small but significant difference is attributed to the difficulties in deprotoning the TiO_2 positive surface due to the presence of the negatively charged SDS molecules which changes the acid–base properties of the TiO_2 surface groups. By increasing further the pH (pH ≥ 10) a continuous decrease of the mean z-average diameters is observed. The sizes of such agglomerates are greater than those of agglomerates formed at pH 3.1 or agglomerates formed at pH 10 by punctual addition (Fig. 1). This is due to the successive pH adjustment and the fact that once formed, large agglomerates only undergo partial disagglomeration. High pH values result in charge inversion to negative values which are close to the values obtained in the absence of surfactants hence indicating desorption of the negatively charged surfactants from the negatively charged ENP surfaces. Under such conditions of low SDS concentration, the TiO_2–SDS complex properties and its pH charge dependency are mainly controlled by the TiO_2 surface properties.

ζ potential values and z-average diameters of TiO_2–SDS complexes formed at 200 mg L^{-1} SDS concentration are presented in Fig. 5b. At pH 3.1 the complexes are negatively charged and the pH increase rapidly results in a decrease of the ζ potential and concomitant formation of agglomerates. Such a behavior is related here to SDS molecule desorption when positive surface sites are deprotonated as well as the

presence of both positive and negative sites on the ENP surface when the ζ potential is equal to zero. The IEP is obtained here at pH 5.2 and corresponds to a state where the number of hydroxyl positive surface sites is still important but exactly counterbalanced by the adsorbed SDS molecules. Further pH increase, from pH 6 to 10, induces TiO_2 surface site deprotonation and a continuous decrease to more negative values of the ζ potential. The size of the agglomerates increases continuously with pH increase from 3 to 8.5 then stabilization is observed. No significant disagglomeration is observed.

Size and surface charge evolution as a function of pH for TiO_2–SDS complexes obtained with an important excess of surfactants (SDS concentration equal to 1442 mg L^{-1}) is represented in Fig. 5c. In the full pH domain, the complexes are found stable with constant z-average diameters and ζ potential values of about 370 nm and −34 mV, respectively. Data indicate here that the SDS–TiO_2 properties are essentially controlled by the presence of the surfactants and that the TiO_2 surface deprotonation has little effect on the complex total charge which is held constant by the desorption of SDS molecules. An excess of SDS molecules in comparison with the experiment previously discussed in the presence of 200 mg L^{-1} prevents a decrease of the ζ potential value upon pH variation and therefore formation of large agglomerates.

The TiO_2–SDS complexes, relative charges, number of SDS molecules and stability diagram with pH have been
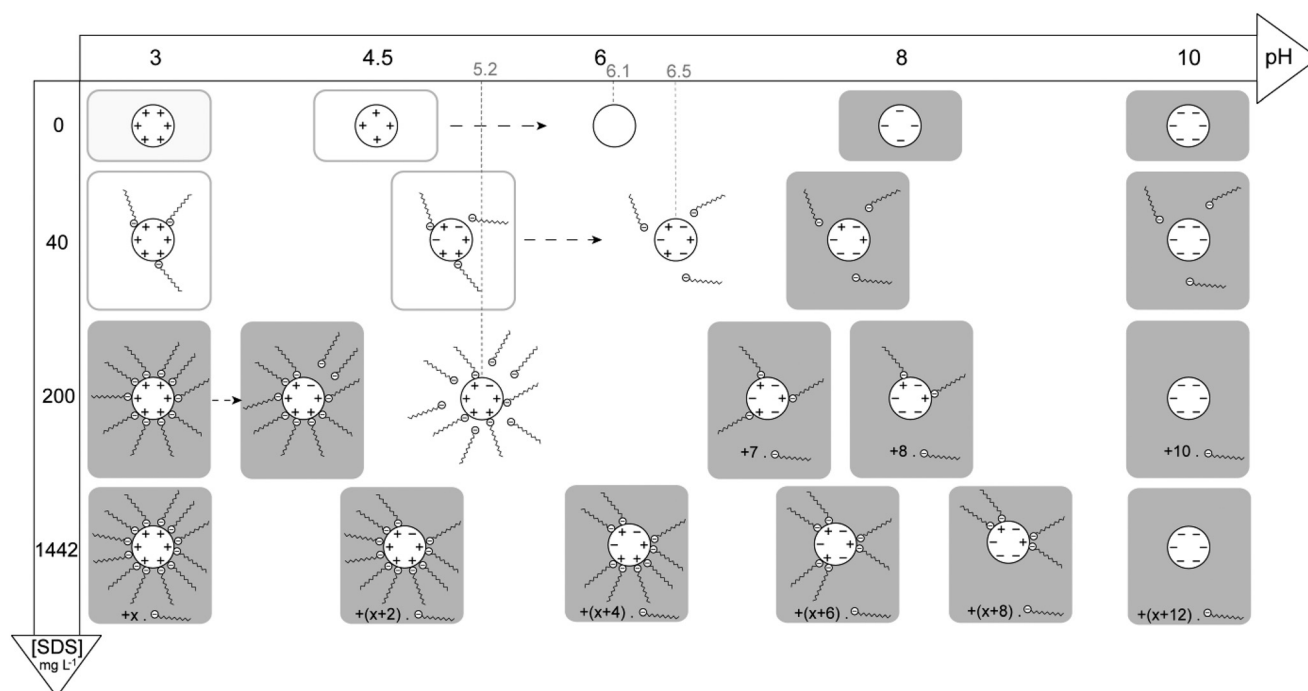
Fig. 6 Stability diagram of TiO_2 and TiO_2–SDS complexes as a function of pH and for different SDS concentrations. In the absence of SDS and for a SDS concentration equal to 40 mg L^{-1} the complexes are positively charged at low pH (empty square). pH increases lead to surface hydroxyl site deprotonation (and SDS desorption), surface charge neutralization (isoelectric point; without square), and agglomeration (dot arrow) until charge inversion is achieved (gray squares representing negative surface charges). At 200 mg L^{-1} agglomeration is observed in most cases as well as SDS desorption due to the decrease of the positive surface charges with pH increase. At 1442 mg L^{-1}, TiO_2–SDS complexes are found stable and negatively charged in the full pH domain. Bold numbers refer to the relative numbers of free surfactants and x to the relative number of free surfactants in the presence of an excess of surfactants (at 1442 mg L^{-1}). [TiO_2] = 50 mg L^{-1}.

208 | *Environ. Sci.: Nano*, 2017, **4**, 203–211

This journal is © The Royal Society of Chemistry 2017

summarized in Fig. 6. The number of charges on TiO_2 ENPs and number of SDS molecules are only qualitative to take into account the total surface charge of the ENPs with respect to the experimental ζ potential values. This stability diagram denotes the subtle interplay between the TiO_2 ENP surface charge, pH, SDS concentration and impacts on SDS adsorption, SDS desorption, agglomeration as well as disagglomeration processes.

3.3. Stability of TiO_2–SDS complexes in the presence of divalent cations and at environmental pH

The stability of TiO_2–SDS complexes is investigated by first forming electrostatic and stable complexes at pH 3.1 and then by introducing them in synthetic water at pH 8.2, with $[Ca^{2+}] = 45$ mg L^{-1} and $[Mg^{2+}] = 5$ mg L^{-1} so as to take into account water hardness. ζ potential value and z-average diameter evolutions as a function of time for different initial SDS concentrations are represented in Fig. 7. In the absence of SDS, when positively charged TiO_2 ENPs are introduced in the synthetic water (Fig. 7a), TiO_2 charge inversion is observed and the ζ potential rapidly changes from a positive value to −7 mV. It should be noted here that this final ζ potential value is lower than that observed in the absence of divalent cations (ζ potential equal to −30 mV at pH 8.2 as shown in Fig. 1). Such a difference is explained by the specific adsorption of divalent cations on the ENP surface in addition to charge screening. Owing to the ζ potential value, large agglomerates are then rapidly formed and, after 30 min, a steady state is obtained. The presence of divalent cations is also found to promote the formation of large agglomerates (diameters up to 3 μm) with the help of cation bridging as represented in Fig. 4b and in comparison with agglomerate diameters obtained in the absence of divalent electrolytes (around 1 μm at pH_{PZC} after 30 min).

For a 40 mg L^{-1} SDS concentration (Fig. 7b) similar trends are observed. However, the final ζ potential values are found more negative in the presence of SDS (−13 versus −7 mV). Under such conditions Ca^{2+} and Mg^{2+} ions are assumed to form complexes with the SDS molecules and, as a result, less divalent cations are available for specific adsorption on TiO_2 surfaces.

For a 200 mg L^{-1} SDS concentration (Fig. 7c) the ζ potential stabilization takes a longer time (90 min instead of 30 min in the previous experiment) due to TiO_2 surface charge modification and equilibrium time between SDS desorption and SDS–cation complex formation. Indeed, we start with a negative surface potential which rapidly becomes positive then decreases again to negative values. The ζ potential plateau obtained here is higher than that obtained in the absence of divalent cations for an identical pH (−25 versus −20 mV in Fig. 5b) as SDS–cation complex formation reduces the SDS amount adsorbed. Finally, for the highest SDS concentration investigated (1442 mg L^{-1}, Fig. 7d) a significant increase of the z-average diameter is observed, if comparison is made in the absence of cations, due to cation bridging between
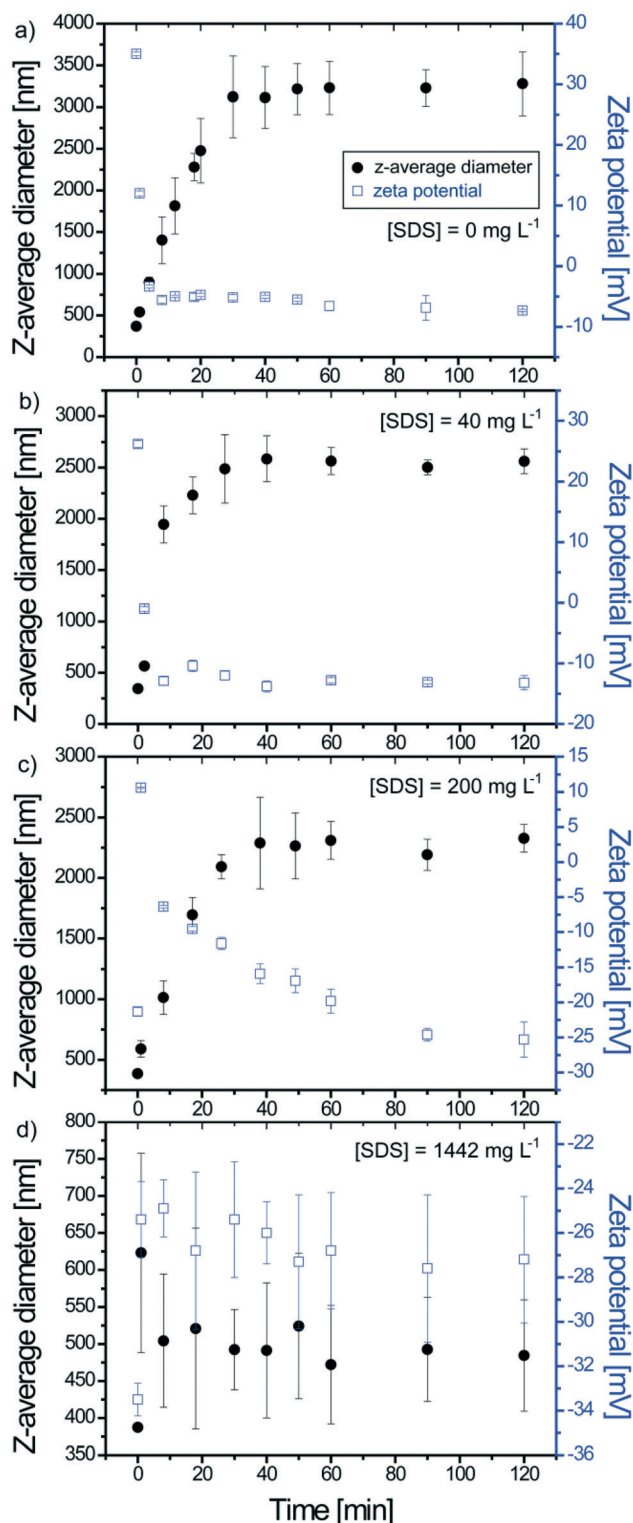

Fig. 7 Z-average diameter and ζ potential value variations as a function of time after pH change from 3.1 (stable complexes) to 8.2 and in the presence of 45 mg L^{-1} Ca^{2+} and 5 mg L^{-1} Mg^{2+} to mimic the effect of water hardness. Strong destabilization is observed for SDS concentrations below or equal to 200 mg L^{-1} (a–c) whereas at a SDS concentration equal to 1442 mg L^{-1} the complexes are found stable. Data indicate the importance of the pH change and the presence of divalent cations on TiO_2–SDS stability and surface charge modifications. $[TiO_2] = 50$ mg L^{-1}, (a) $[SDS] = 0$ mg L^{-1}, (b) 40 mg L^{-1}, (c) 200 mg L^{-1} and (d) 1442 mg L^{-1}.
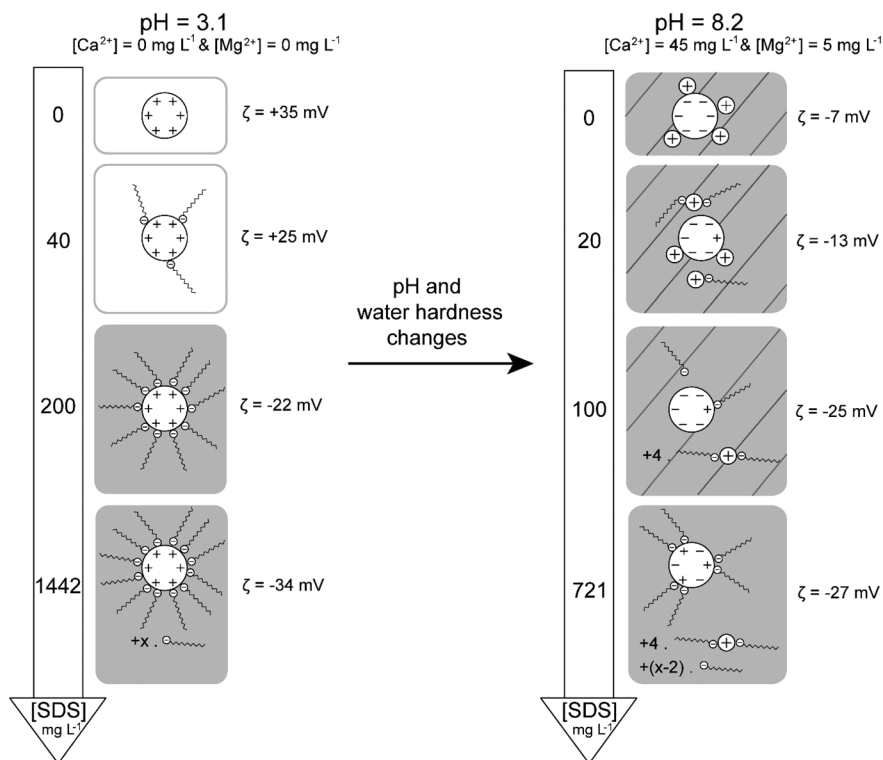
Fig. 8 Schematic illustration of TiO_2–SDS complex behavior after an important pH change and in the presence of divalent cations. Divalent cations ($\oplus$) strongly influence not only the ENP surface charge due to specific adsorption but also the SDS molecule behavior in the bulk *via* complexation processes. Hashed squares represent destabilized TiO_2–SDS complexes. Empty or grey squares represent respectively positively and negatively charged surfaces. $[TiO_2]$ = 50 mg L^{-1}.

TiO_2–SDS complexes as represented in Fig. 4c. The ζ potential reaches a constant value equal to −27 mV which is lower than that observed in the absence of Ca^{2+} and Mg^{2+} (−34 mV at pH 8.2) due to SDS–cation complex formation. Less SDS molecules are then available for adsorption on the TiO_2 surface. Fig. 8 summarizes the influence of the pH change and the presence of divalent cations on the resulting stability and structure of TiO_2–SDS complexes. Agglomeration conditions are presented in this figure by hatched squares.

4. Conclusion

In this study, using a mechanistic approach, we demonstrate that surfactant molecules can significantly influence ENP stability through several processes. The surfactant concentration, mixing procedure (punctual or successive addition), pH as well as the presence of divalent cations are also found to be of high importance.

Stabilization/destabilization processes are shown here to be governed by complex mechanisms such as electrostatic repulsions, hydrophobic interactions between SDS chains, specific adsorption of divalent cations, adsorption/desorption of surfactant molecules, and cation bridging. It should be also noted that for a given SDS concentration, electrostatic TiO_2–SDS complexes can undergo important transformation with pH. We believe that this study is of high value for i) the design of ENP dispersion protocols to improve nanoparticle sta-

bility with the use of surfactant molecules, ii) a better understanding of ENP commercial dispersions stabilized by surfactants in contact with environmental matrices, iii) the understanding of the impact of water hardness on the SDS–TiO_2 nanoparticle interactions in particular by considering the competition between the divalent cations, surfactant molecules and TiO_2 nanoparticles, and iv) for risk assessment evaluation of ENPs entering aquatic systems where both changes in pH and water hardness are expected.

Acknowledgements

References

1 M. Auffan, J. Rose, J.-Y. Bottero, G. V. Lowry, J.-P. Jolivet and M. R. Wiesner, *Nat. Nanotechnol.*, 2009, **4**, 634–641.
2 X. Chen and S. S. Mao, *Chem. Rev.*, 2007, **107**, 2891–2959.
3 A.-H. Lu, E. L. Salabas and F. Schueth, *Angew. Chem., Int. Ed.*, 2007, **46**, 1222–1244.
4 X. L. Luo, A. Morrin, A. J. Killard and M. R. Smyth, *Electroanalysis*, 2006, **18**, 319–326.

210 | *Environ. Sci.: Nano*, 2017, **4**, 203–211

This journal is © The Royal Society of Chemistry 2017

5   C. O. Hendren, X. Mesnard, J. Droege and M. R. Wiesner, *Environ. Sci. Technol.*, 2011, **45**, 2562–2569.

6   K. Schmid and M. Riediker, *Environ. Sci. Technol.*, 2008, **42**, 2253–2260.

7   F. Piccinno, F. Gottschalk, S. Seeger and B. Nowack, *J. Nanopart. Res.*, 2012, **14**, 1109.

8   M. Gratzel, *J. Photochem. Photobiol., A*, 2004, **168**, 235.

9   A. Weir, P. Westerhoff, L. Fabricius, K. Hristovski and N. von Goetz, *Environ. Sci. Technol.*, 2012, **46**, 2242–2250.

10 B. Mahltig, H. Bottcher, K. Rauch, U. Dieckmann, R. Nitsche and T. Fritz, *Thin Solid Films*, 2005, **485**, 108–114.

11 P. D. Cozzoli, R. Comparelli, E. Fanizza, M. L. Curri and A. Agostiano, *Mater. Sci. Eng., C*, 2003, **23**, 707–713.

12 X. Jimin, J. Deli, C. Min, L. Di, Z. Jianjun, L. Xiaomeng and Y. Changhao, *Colloids Surf., A*, 2010, **372**, 107–114.

13 R. A. French, A. R. Jacobson, B. Kim, S. L. Isley, R. L. Penn and P. C. Baveye, *Environ. Sci. Technol.*, 2009, **43**, 1354–1359.

14 R. F. Domingos, C. Peyrot and K. J. Wilkinson, *Environ. Chem.*, 2010, **7**, 61–66.

15 B. Mukherjee and J. W. Weaver, *Environ. Sci. Technol.*, 2010, **44**, 3332–3338.

16 J. A. Gallego-Urrea, J. Perez Holmberg and M. Hassellov, *Environ. Sci.: Nano*, 2014, **1**, 181–189.

17 M. Baalousha, A. Manciulea, S. Cumberland, K. Kendall and J. R. Lead, *Environ. Toxicol. Chem.*, 2008, **27**, 1875–1882.

18 M. Erhayem and M. Sohn, *Sci. Total Environ.*, 2014, **468–469**, 249–257.

19 O. Spalla, *Curr. Opin. Colloid Interface Sci.*, 2002, **7**, 179–185.

20 E. Bae, H.-J. Park, J. Park, J. Yoon, Y. Kim, K. Choi and J. Yi, *Bull. Korean Chem. Soc.*, 2011, **32**, 613–619.

21 M. D. Clark, S. Subramanian and R. Krishnamoorti, *J. Colloid Interface Sci.*, 2011, **354**, 144–151.

22 K. Holmberg, *J. Colloid Interface Sci.*, 2004, **274**, 355–364.

23 L. R. Parent, D. B. Robinson, T. J. Woehl, W. D. Ristenpart, J. E. Evans, N. D. Browning and I. Arslan, *ACS Nano*, 2012, **6**, 3589–3596.

24 G. G. Ying, *Environ. Int.*, 2006, **32**, 417–431.

25 http://www.cefic.org/About-us/How-Cefic-is-organised/Fine-Speciality-and-Consumer-Chemicals/Comite-European-des-Agents-de-Surface-CESIO-/- (Accessed July 13, 2016).

26 E. Samper, M. Rodriguez, M. A. De la Rubia and D. Prats, *Sep. Purif. Technol.*, 2009, **65**, 337–342.

27 X. Li, G.-M. Zeng, J.-H. Huang, C. Zhang, Y.-Y. Fang, Y.-H. Qu, F. Luo, D. Lin and H.-L. Liu, *J. Membr. Sci.*, 2009, **337**, 92–97.

28 T. Imae, K. Muto and S. Ikeda, *Colloid Polym. Sci.*, 1991, **269**, 43–48.

29 C. Arnold, S. Ulrich, S. Stoll, P. Marie and Y. Holl, *J. Colloid Interface Sci.*, 2011, **353**, 188–195.

30 Y. Liu, M. Tourbin, S. Lachaize and P. Guiraud, *Chemosphere*, 2013, **92**, 681–687.

31 Y. Liu, M. Tourbin, S. Lachaize and P. Guiraud, *Ind. Eng. Chem. Res.*, 2012, **51**, 1853–1863.

32 C. Y. Lien and J. C. Liu, *J. Environ. Eng.*, 2006, **132**, 51–57.

33 C. Y. Hu, S. L. Lo, C. M. Li and W. H. Kuan, *J. Hazard. Mater.*, 2005, **120**, 15–20.

34 H. Li and C. P. Tripp, *Langmuir*, 2004, **20**, 10526–10533.

35 S. Mehan, V. K. Aswal and J. Kohlbrecher, *Langmuir*, 2014, **30**, 9941–9950.

36 S. Mehan, A. J. Chinchalikar, S. Kumar, V. K. Aswal and R. Schweins, *Langmuir*, 2013, **29**, 11290–11299.

37 K. P. Sharma, V. K. Aswal and G. Kumaraswamy, *J. Phys. Chem. B*, 2010, **114**, 10986–10994.

38 B. Cattoz, T. Cosgrove, M. Crossman and S. W. Prescott, *Langmuir*, 2012, **28**, 2485–2492.

39 N. Sani-Kast, M. Scheringer, D. Slomberg, J. Labille, A. Praetorius, P. Ollivier and K. Hungerbuhler, *Sci. Total Environ.*, 2015, **535**, 150–159.

40 G. E. Batley, J. K. Kirby and M. J. McLaughlin, *Acc. Chem. Res.*, 2013, **46**, 854–862.

41 F. Gottschalk, T. Sonderer, R. W. Scholz and B. Nowack, *Environ. Sci. Technol.*, 2009, **43**, 9216–9222.

42 S. M. Louie, R. D. Tilton and G. V. Lowry, *Environ. Sci.: Nano*, 2016, **3**, 283–310.

43 G. Cornelis, *Environ. Sci.: Nano*, 2015, **2**, 19–26.

44 E. Goldberg, M. Scheringer, T. D. Bucheli and K. Hungerbuhler, *Environ. Sci.: Nano*, 2015, **2**, 352–360.

45 B. Collin, M. Auffan, A. C. Johnson, I. Kaur, A. A. Keller, A. Lazareva, J. R. Lead, X. Ma, R. C. Merrifield, C. Svendsen, J. C. White and J. M. Unrine, *Environ. Sci.: Nano*, 2014, **1**, 533–548.

46 L. R. Pokhrel, B. Dubey and P. R. Scheuerman, *Environ. Sci.: Nano*, 2014, **1**, 45–54.

47 A. Biswal, B. C. Tripathy, T. Subbaiah, D. Meyrick and M. Minakshi, *J. Electrochem. Soc.*, 2015, **162**, 30–38.

48 J. S. Taurozzi, V. A. Hackley and M. R. Wiesner, *National Institute of Standards and Technology Special Publication*, 2012, pp. 1200–1203.

49 M. Baalousha, *Sci. Total Environ.*, 2009, **407**, 2093–2101.

50 H. Ohshima, *Adv. Colloid Interface Sci.*, 1995, **62**, 189–235.

51 G. A. Parks, *Chem. Rev.*, 1965, **65**, 177–198.

52 A. Praetorius, J. Labille, M. Scheringer, A. Thill, K. Hungerbuehler and J.-Y. Bottero, *Environ. Sci. Technol.*, 2014, **48**, 10690–10698.

53 B. Faure, G. Salazar-Alvarez, A. Ahniyaz, I. Villaluenga, G. Berriozabal, Y. R. De Miguel and L. Bergstrom, *Sci. Technol. Adv. Mater.*, 2013, **14**, 023001.

54 A. M. Khan and S. S. Shah, *J. Chem. Soc. Pak.*, 2008, **30**, 186–191.

55 A. Cifuentes, J. L. Bernal and J. C. DiezMasa, *Anal. Chem.*, 1997, **69**, 4271–4274.

This journal is © The Royal Society of Chemistry 2017

Environ. Sci.: Nano, 2017, **4**, 203–211 | 211